

# Structural Analysis of Thin Ni-P Layers

PETRICĂ ALEXANDRU<sup>1\*</sup>, TAMARA RADU<sup>2</sup>, FLORENTINA POTECASU<sup>1</sup>, MARIA VLAD<sup>2</sup>, GINA GENOVEVA ISTRATE<sup>2</sup>, DANIELA L. BURUIANA<sup>2\*</sup>, BOGDAN-GABRIEL CARP<sup>3</sup>

<sup>1</sup>Dunarea de Jos University of Galati, Department of Science and Materials Engineering, 111 Domneasca Str., 800201, Galati, Romania,

<sup>2</sup>Dunarea de Jos University of Galati, Department of Environmental and Security Engineering in Industry, 111 Domneasca Str., 800201, Galati, Romania,

<sup>3</sup>Dunarea de Jos University of Galati, Department of Thermal Systems and Environmental Engineering, 111 Domneasca Str., 800201, Galati, Romania

*The deposition mechanism by autocatalytic reduction method is a chemical one, which does not lead to structures as shown in the Ni-P balance diagram. In the experiments of the present work, Ni-P layers were made deposited on thin steel strip with low carbon content. By optical microscopy and scanning electron microscopy by (SEM) it was analyzed the appearance and surface morphology of the deposited layers depending on the content of phosphorus and working parameters (temperature, pH, stirring speed). The layer structure was analyzed in the cross section and on the break surface. The analysis results show that thin coatings of Ni-P have a surface topography that follows faithfully the steel support. Depending on the content of phosphorus, on the layer surface of low phosphorus content, spherical particles of different sizes can be seen while high and average phosphorus content coatings feature a smooth surface with nanometer-sized grains. Analysis of the cut-off /break section of the Ni-P layer structure, show a more or less porous structure depending on the stirring speed and pH level.*

**Keywords:** Ni-P layers; electroless method; autocatalytic reduction, optical microscopy, SEM, adhesion by Erichsen test.

Depending on the content of phosphorous, the electroless deposition of Ni-P may have crystalline, amorphous or mixed structure. [1, 2]. Deposits with low phosphorus content (1-5% P) are crystalline; those with average phosphorus content (from 6 to 9%) have mixed structures made up of areas of crystalline and amorphous structures and coatings with high phosphorus content (10-13% P) are amorphous [3, 4].

According to the Ni-P balance diagram [5], below the solidus temperature, in the Ni-P alloy there is a phase  $\alpha$ , which is a solid solution of Ni with 0.17 wt.% P, and the intermetallic compound Ni<sub>3</sub>P, which contains 15 wt.% P. The region between these single-phase areas consists of a two-phase mixture,  $\alpha$  and Ni<sub>3</sub>P.

Structural analyzes carried out and presented in the literature show that Ni-P layers deposited by autocatalytic reduction method have out of balance structures. The out of balance phase diagram of the Ni-P alloy has two additional steps which are not in the balance diagram:  $\beta$  phase, a crystalline solution of phosphorus in nickel (4.5 wt. % P); and  $\gamma$  phase, a totally amorphous phase with a content of 11 to 15 wt. % phosphorus. Between the areas of the existence of these two phases there is a two-phase region corresponding to the concentration range from 4.4 to 11.0 wt. %P, in which both phases  $\beta$  and  $\gamma$  coexist [3].

The balance structures cannot form because the intermetallic compounds such as Ni<sub>3</sub>P do not arise from the chemical reactions that occur during the electroless deposition. For the Ni<sub>3</sub>P balance phase to form it would be

necessary that a large number of atoms move by diffusion to the deposition surface (three nickel atoms for a phosphorus one), a process which is not possible under the concrete conditions of electroless deposition. Phosphorus atoms are included among the nickel atoms resulting from the electrochemical process, supersaturating the crystal lattice of nickel [6].

Nickel crystallizes in face-centered cubic system (fcc), each atom having other 12 close neighbors. Capturing phosphorous into the nickel structure prevents the arrangement of atoms in the fcc network over long distances, thus resulting very small dimensions of the crystalline grains. With increased phosphorus content fcc ordering cannot be maintained and the structures becomes semi-crystalline or even amorphous [7, 8].

The literature shows the structural characterization of consistent Ni-P layers, 20-25 $\mu$ m, obtained at higher immersion times of 1-3 h [9-11]. As practical applications of electroless process are productive at much less times, this paper aims to characterize thin films of Ni-P, less studied, obtained at immersion durations of 5-15 min able to ensure protection of the steel support, for applications such as decorative or work in less aggressive environments [12,14].

## Experimental part

### Materials and methods

Deposition of Ni-P layers was performed on thin steel strips (0.18 mm) of a chemical composition as shown in table 1.

**Table 1**  
CHEMICAL COMPOSITION OF THE SUPPORT STRIPS STEEL

| C     | Si    | Mn    | P     | S    | Al    | As    | Ti    | V     | Cu    | Ni    | Cr    | Mo    |
|-------|-------|-------|-------|------|-------|-------|-------|-------|-------|-------|-------|-------|
| [%]   | [%]   | [%]   | [%]   | [%]  | [%]   | [%]   | [%]   | [%]   | [%]   | [%]   | [%]   | [%]   |
| 0.025 | 0.015 | 0.210 | 0.013 | 0.01 | 0.046 | 0.004 | 0.002 | 0.001 | 0.005 | 0.008 | 0.025 | 0.001 |

\* email: petrica.alexandru@ugal.ro; dnegoita@ugal.ro

| pH      | T [°C] | Process duration [min] | Stirring rate [rot/min] |
|---------|--------|------------------------|-------------------------|
| 3.8-6.6 | 83±1   | 5, 10, 15              | 200-300                 |

Preparation of samples means [13]:  
 - Chemical degreasing at 80-90 °C, followed by two washings in hot water (85-90 °C);  
 - Pickling in hydrochloric acid, 20% solution and washing in warm water at nickel bath temperature.

Layers were obtained in a bath of 24 [g/L] nickel sulfate 20 [g/L], sodium hypophosphite 9 [g/L] sodium acetate and 0.001 [g/L] lead acetate.

The parameters tested are shown in table 2.

## Results and discussions

### EDX analysis of Ni-P layers

The equipment used was an electron microscope FEI Quanta 200 (produced in Czech Republic) fitted with an X-ray analyzer under an angle of 45°, from the position of the sample inside the microscope.

Samples nickel coated at 83-84°C were analyzed under 10 min deposition time and bath stirring at 200rot/min, at different pH values respectively: 5.92; 4.95 and 3.81. Table 3 shows the results of EDX analysis

**Table 3**  
THE RESULTS OF EDX ANALYSIS

| pH   | Chemical composition, [wt%] |       |       |
|------|-----------------------------|-------|-------|
|      | P                           | Ni    | Fe    |
| 5.92 | 4.84                        | 90.75 | 2.68  |
| 4.95 | 9.53                        | 85.83 | 4.46  |
| 3.81 | 12.42                       | 69.84 | 17.74 |

EDX spectrum (fig. 1) indicates the presence of nickel and phosphorus and also elements of the steel substrate, especially iron, because the depth of the beam penetration exceeded the deposited layer thickness.

EDX analysis results confirm data from literature [3, 7] i.e. increase of the phosphorus content when decreasing the pH level. Decreasing the pH slows down the reduction

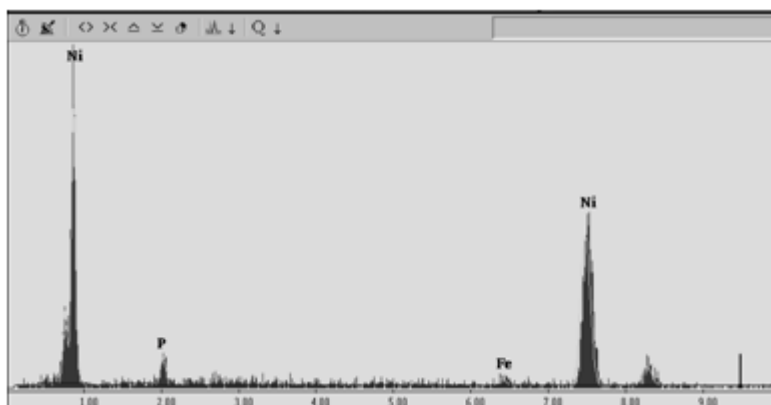


Fig.1. Results of EDX analysis on Ni-P layer obtained at pH=5.92.

**Table 2**  
WORKING PARAMETERS USED IN OBTAINING THE COATINGS

reaction of Ni<sup>2+</sup> ions decreasing the rate of Ni deposition and favoring the deposition of phosphorus. During the process of nickel coating, the pH decreases continuously faster or slower depending on the effectiveness of the buffers and bath stirring. Adjusting the pH values to the values studied was done with NaOH alkaline solutions and acid solutions of acetic acid.

### XRD Analysis

The analysis by diffractometry (XRD) enables identification of the phases present in the layer, crystallinity of the structure, crystals size and internal tensions.

Samples were subjected to X-ray by type Cu K $\alpha$  to a scan speed of 0.5 [deg/min]. From the diffraction diagrams two peaks at  $2\theta = 44.78$  were highlighted, corresponding to the orientation of Ni (111) and at  $2\theta = 65.04$  corresponding to the iron in the substrate, visible due to the small layer thickness (fig. 2). For diffraction shown in figure 2, the large surface area corresponding to peak Ni (111) show the formation of semi-crystalline structures. Grain size, calculated using Williamson Hall method, ranged between 170 and 126 nm. Maximum deviation relative to the crystal lattice parameter, in relation to average thickness varied between 1.68 and 1.93%.

### Surface Morphology

Ni-P coating surface morphology was studied by macroscopic analysis, optical microscopy and SEM. Macroscopically the coated samples have an attractive / decorative metallic- shiny aspect. Samples obtained at high pH feature a somewhat rougher surface than the other. Both types of microscopic analysis showed, according to the phosphorus content, a different aspect of the layers surface (fig. 3 and 4). The coatings with low phosphorus content (3a and 4a.) show a surface of almost spherical

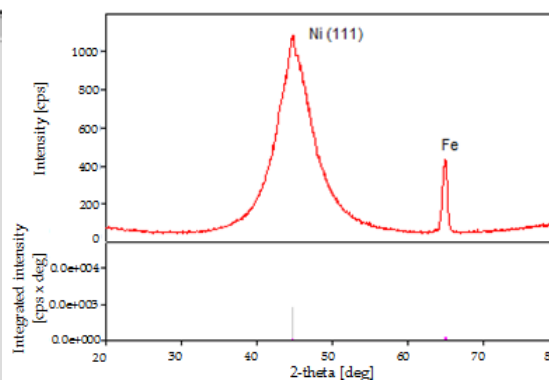


Fig. 2. XRD pattern of Ni-P deposits on steel, obtained at 84°C, 15min, pH=4.95.

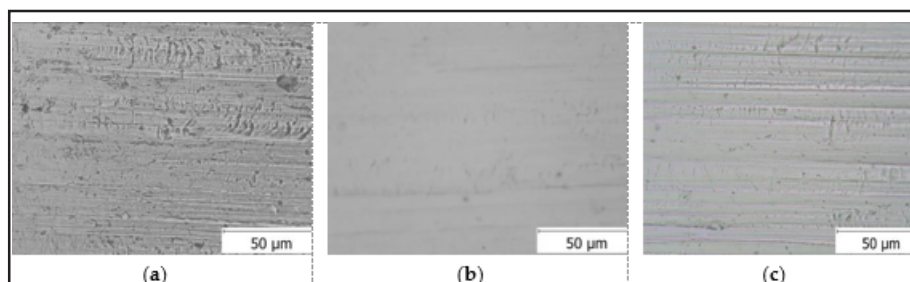


Fig. 3. Optical micrographs of Ni-P coatings surface depending of the phosphorus content. a) 4.84%P. b) 9.53%P. c) 12.42% P.

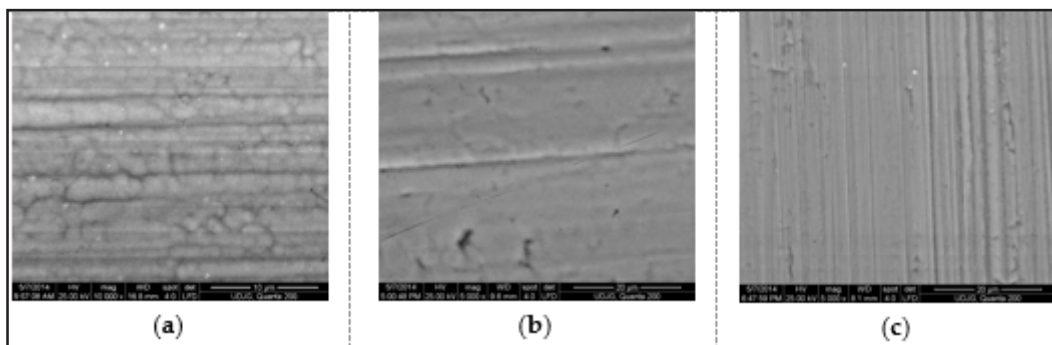


Fig. 4. SEM morphology of Ni-P coatings depending of the phosphorus content. a) 4.84%P. b) 9.53%P. a) 12.42% P.

grains of different sizes while coatings with medium and high phosphorus content have a fine-grained uniform size surface (fig. 3b and c and fig. 4b and c). SEM morphological analysis of the Ni-P thin films was carried out in low vacuum mode, using the secondary electron detector at a pressure of 60 Pa. The electron accelerating voltage was 25 kV and the electron beam spot of 4 (arbitrary units).

The samples presented in figure 3 were obtained at 15 min and have a 7-10 $\mu$ m layer thickness and those in figure 4 for a time of 10 min and have a thickness of 2.5 - 4.5 $\mu$ m.

It is also found that the degree of the steel support finishing and the layer thickness affects the appearance of the layer surfaces, at the same content of phosphorus in the layer, as highlighted in figure 5-7. The Ni-P thin films obtained at short durations of immersion, up to 5 minutes (fig. 5a, 6a, 7a) enable to observe the support roughness, namely the steel strip obtained by cold rolling and drawing, with a thickness of 0.18 mm. For samples immersed for 15 min in the electroless bath (fig. 5b, 6b, 7b), especially at high pH (fig. 5b, 6b), it can be seen, besides the arrangement of bold strings (corresponding to the band grooves) an increase in grain as well.

Structural analyses by optical microscopy and electron microscopy highlight, on the surface of samples with low phosphorus content, the presence of nickel nodules of nearly spherical shapes as shown in figure 8.

The literature mentions that these nodules are typical for the amorphous structure [9, 16].

#### Ni-P Layer Microstructure Analysis

The analysis of the break section of the layers at an angle of 30° reveals a high porosity structure. In [15] it is shown that the layers below 10 $\mu$ m in size, as is the case concerned, show high porosity, the minimum porosity reaching a 25 $\mu$ m layer thickness. In addition to the layer thickness, porosity is strongly influenced by the substrate surface characteristics (such as roughness and morphology) and the electroless bath stirring [18,19]. The pores are formed mainly due to the incorporation of hydrogen (resulting from chemical reactions) and an optimal stirring (air bubbling) can provide its advanced elimination and lower porosity. Analysis of pores in the break section of Ni-P layers and to increasingly larger values shows they do not communicate with the surface of the steel layer (fig. 9) and the surface of the Ni-P layer (fig. 10).

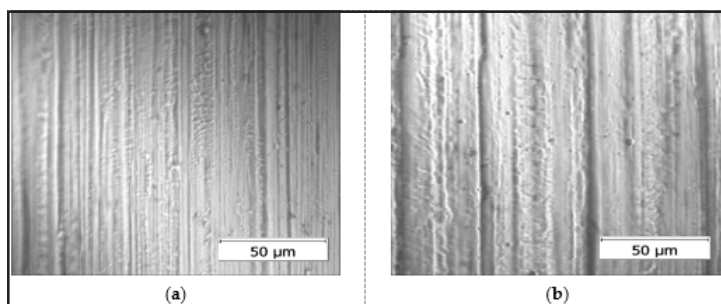


Fig. 5. Aspect of the Ni P layer surface vs deposition time (layer thickness), obtained at pH=5.92 and 83°C. a) 5 min. b) 15 min.

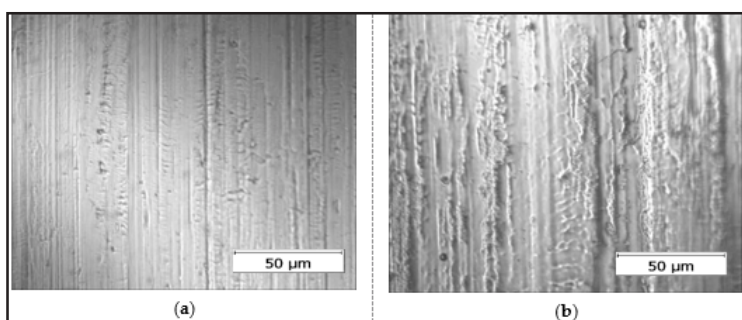


Fig. 6. Aspect of the Ni P layer surface vs deposition time (layer thickness), obtained at pH=4.95 and 83°C a) 5 min. b) 15 min.

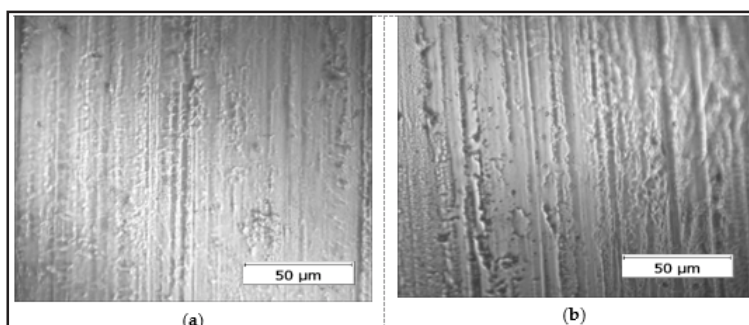


Fig. 7. Aspect of the Ni P layer surface vs deposition time (layer thickness), obtained at pH=3.81 and 83°C. a) 5 min. b) 15 min.

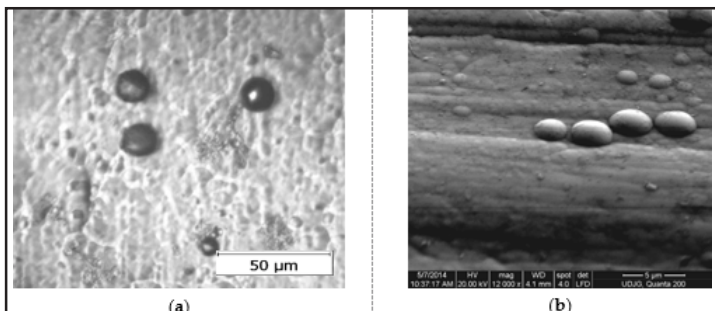


Fig. 8. Morphology of low phosphorus content layer surface - 4.84% P a) Optical microscopy. b) SEM.

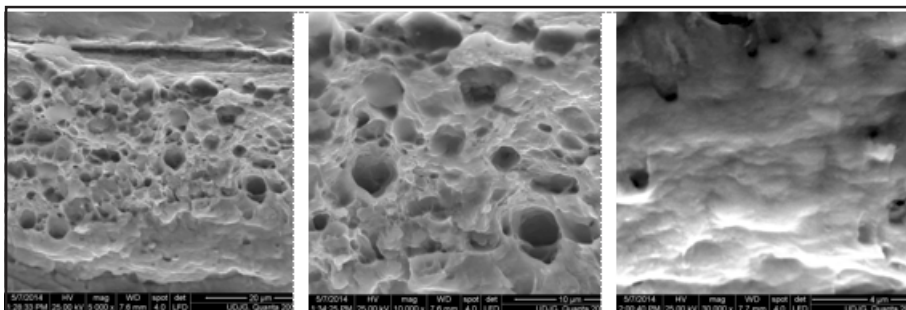


Fig. 9. SEM micrographs at various thicknesses of Ni-P layer in the break section.

The Ni-P layer presented in figure 9 has been obtained by immersing for 10 min. in electroless bath of a 5.92 pH under magnetic stirring to 200rot/min and a temperature of about 83°C.

Under the present experiment it can be seen a reduction in porosity with a decreased pH, as shown in figure 10. Such an influence of the pH on the porosity of Ni-P layer is also observed in [17]. Decreasing pH slows the reactions specific to electroless process and hence the formation of molecular hydrogen which by layer embedding forms pores.

SEM analysis in the break section of the Ni-P layer has also allowed the layer thickness measurement. As seen in figure 11, layer thickness decreases significantly with lower pH from 5.92 to 4.95 (3.5 to 4.6μm from the 2.7-2.2μm). Lowering pH below 4 no longer significantly influence the layer thickness thus resulting a thickness of about 2μm.

SEM analysis in the break section of the Ni-P layer has also allowed the layer thickness measurement. As seen in

figure 11, layer thickness decreases significantly with lower pH from 5.92 to 4.95 (3.5 to 4.6μm from the 2.7-2.2μm). Lowering pH below 4 no longer significantly influence the layer thickness thus resulting a thickness of about 2μm. In the break section a fibrous structure is observed at 5.92 pH level (11a) and a stratified structure at pH 4.95 (fig. 11b).

The cross-section analysis of the sample microstructure made under different conditions of pH (fig. 12) shows also a decrease in the layer thickness with lower pH [20]. Lowering the pH makes the deposition process very slow resulting in lower layer thicknesses for the same period of exposure (12a, 12b).

At higher magnification, made by SEM microscopy, it can be seen on thick layers (fig. 12c) a structure in horizontal bands (laminar structure of the deposited layer as observed in fig. 11b). This structure reveals a difference in the chemical composition over the layer height possible due to the specific mechanism of co-deposition of the nickel and phosphorous ions.

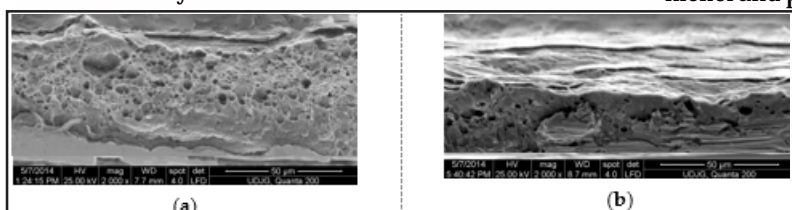


Fig. 10. SEM micrographs of the Ni-P layer in the break section under a beveling angle of 30°. a) pH=5.92, 10 min. b) pH=4.95, 10 min.

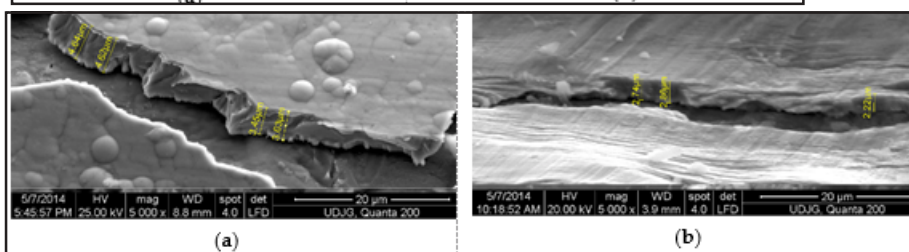


Fig. 11. Variation of layer thickness with the pH of the electroless bath for 10 min duration and a temperature of 83°C. a) pH=5.92. b) pH=4.95.

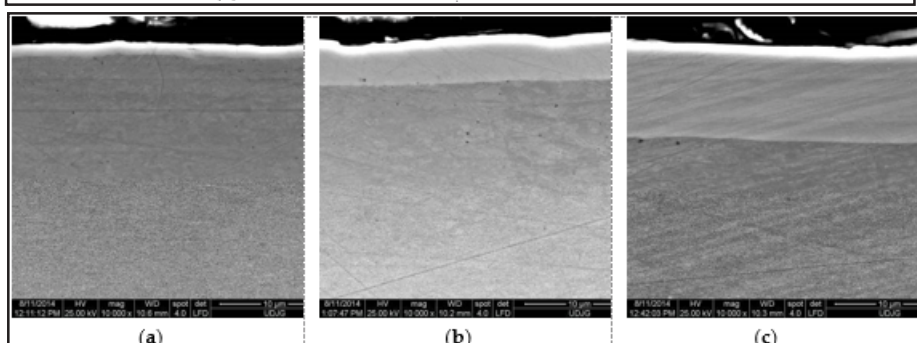


Fig. 12. SEM micrographs of cross-section of Ni-P layers electroless deposited, duration 15 min. and temperature 83°C. a) pH=3.81. b) pH=4.95. c) pH=5.92

## Conclusions

Thin films of 2-7 $\mu$ m Ni-P deposited on cold rolled thin strip were analyzed. The support strip shows parallel burrs from machining that can be observed microscopically even after nickel deposit, regardless of the operating parameters.

Samples immersed for 15 min, especially those obtained at high pH, besides having pronounced row arrangement (corresponding to the band roughness) also feature an increase in layer grains.

The analysis in the break section of thin Ni-P layers, obtained at short exposure of 5-10 min., shows a high porosity structure. Under the present experiment it was observed a reduction of porosity by increased phosphorus content (decreased pH). The structure in the break section is fibrous under successive layers arrangement.

Microstructure analysis reveals uniform layers, in a continuous and clean interface with the support strip. Thick layers can be seen on the laminar structure.

## References

1. BALARAJU, J.N.; KALAVATI; RAJAM, K.S. Influence of particle size on microstructure, hardness and corrosion resistance of electroless Ni-P-Al<sub>2</sub>O<sub>3</sub>, composite coatings. *Surf. & Coat. Technol.* 2006, 200, 3933-3941.
2. BALINT, S.I.; CONSTANTINESCU, S.; BALINT, L. Influence of heat treatment on the characteristics of Ni-P-Al<sub>2</sub>O<sub>3</sub> composite layers. *Proceedings of the 15th International Multidisciplinary Scientific GeoConference SGEM 2015*, Albena, Bulgaria, 18-24, June, 2015.
3. TAHERI, R. Evaluation of Electroless Nickel-Phosphorus (EN) Coatings, PhD Thesis, University of Saskatchewan, Saskatoon, 2003, 13-14.
4. AFROUKHTEH, S.; DEGHANIAN, C.; EMAMY, M. Preparation of electroless Ni-P composite coatings containing nano-scattered alumina in presence of polymeric surfactant. *Progres in Nature Science: Materials International*. 2012, 22(4), 318-325.
5. ASM Handbook vol. 3. Alloy Phase Diagrams. ASM International, USA, 1992, pp. 1216.
6. WEIL, R.; PARKER, K. Properties of Electroless Nickel Plating. In *Electroless Plating: Fundamentals and Applications*, Mallory, G.O.; Hajdu, J.B., American Electroplaters and Surface Finishers Society, Orlando, Florida, USA, 1990, pp. 111.
7. SCHLESINGER, M. Electroless Deposition of Nickel. In *Modern Electroplating*, 5th ed.; Schlesinger M. and Paunovic M., Wiley, USA, 2011, pp. 447-457.
8. KRISHNAN, K.H.; JOHN, S.; SRINIVASAN, K.N.; PRAVEEN, J.; GANESAN, M.; KAVIMANI, P.M. An Overall Aspect of Electroless Ni-P Depositions—A Review Article. *Metallurgical and Materials Transactions A*, 2006, 37A, 1917-1925.
9. SEIFZADHEN, D.; RAJABALIZADEH, Z. Environmentally-friendly method for electroless Ni-P plating on magnesium alloy. *Surface&CoatingsTehnology*, 2013, 218, 119-126.
10. RAVOIU, A., BENE, L., The pH Value Effect Of A Simulated Physiological Solution On The Corrosion Resistance Of Ti-6al-4v Alloy, 17th International Multidisciplinary Scientific GeoConference SGEM 2017, www.sgem.org, SGEM2017 Conference Proceedings, ISBN 978-619-7408-12-6 / ISSN 1314-2704, 29 June - 5 July, 2017, Vol. 17, Is
11. CHEN, W.; GAO, W.; HI, Y. A novel electroless plating of Ni-P-TiO<sub>2</sub> nano-composite coatings. *Surface&CoatingsTehnology*, 2010, 204, 2493-2498.
12. NOVAKOVIC, J.; VASSILIOU, P.; SAMARA, KL.; ARGYROPOULOS, Th. Electroless Ni-P-TiO<sub>2</sub> composite coatings: Their production and properties. *Surfaces&CoatingsTehnology*, 2006, 201, 895-901.
13. RAVOIU, A., BENE, L., CHIRIAC, A., Metabolic Albumin and Its Effect on Electrochemical Behavior of Titanium Implant Alloy, *Materials Science and Engineering* 374 (2018) 012077, doi:10.1088/1757-899X/374/1/012077.
14. MAINIER, B.F.; CINDRA FONSECA, M.P.; TAVARES, S.S.M.; PARDAL, J.M. Quality of Electroless Ni-P (Nickel-Phosphorus) Coatings Applied in Oil Production Equipment with Salinity. *Journal of Materials Science and Chemical Engineering*, 2013, 1, 1-8.
15. BURUIANA, D.L., BALTA, S., ITICESCU, C., GEORGESCU, L., LEFTER, D., Determining the concentration of heavy metals in the soils near slag landfills, pp108-114, 2016, *Revista Romana de materiale* vol 46, (1).
16. BALARAJU, J.N.; ANANDAN, C.; RAJAM, K.S. Morphological study of ternary Ni-Cu-P alloys by atomic force microscopy. *App.Surf.Sci.*, 2005, 250, 88-97.
17. TAHERI, R. Evaluation of Electroless Nickel-Phosphorus (EN) Coatings, PhD Thesis, University of Saskatchewan, Saskatoon, 2003, 40-45.
18. SEVUGAN, K.; SELVAM, M.; SRINIVASAN, K. N.; VASUDEVAN T.; MANISANKAR, P. Effect of Agitation in Electroless Nickel Deposition. *Plating and Surface Finishing*, 1993, 80, 56-58.
19. BURUIANA, D.L., BORDEI, M., SANDU, I.G., CHIRCULESCU, A.I. SANDU, I., Recycling Waste Grit in Mix Asphalt, *Mat.Plast.*, 50, no. 1, 2013, p.36-39.
20. MALLORY, G.O. Compositions and Kinetics of Electroless Nickel Plating. In *Electroless Plating: Fundamentals and Applications*, Mallory, G.O.; Hajdu, J.B., American Electroplaters and Surface Finishers Society, Orlando, Florida, USA, 1990, pp. 72.

Manuscript received: 22.09.2018